Thermal Stability of Ultrathin Cr Films on Pt (111)

ARTICLE *in* THE JOURNAL OF PHYSICAL CHEMISTRY B · JUNE 1997

Impact Factor: 3.3 · DOI: 10.1021/jp9627786

4 AUTHORS, INCLUDING:

Ulrike Diebold
TU Wien
234 PUBLICATIONS **13,179** CITATIONS

Thermal Stability of Ultrathin Cr Films on Pt(111)

Lanping Zhang, Markus Kuhn,* and Ulrike Diebold

Department of Physics, Tulane University, New Orleans, Louisiana 70118

José A. Rodriguez

Department of Chemistry, Brookhaven National Laboratory, Upton, New York 11973

Received: September 10, 1996; In Final Form: January 22, 1997[⊗]

The thermal stability of ultrathin chromium films on Pt(111) has been studied using low-energy He^+ ion scattering spectroscopy, X-ray photoelectron spectroscopy, low-energy electron diffraction, and scanning tunneling microscopy. At room temperature, Cr grows on Pt(111) with a modified Stranski−Krastanov growth mode (almost complete wetting of the first two layers with subsequent three-dimensional island growth). Upon annealing, chromium diffuses into the Pt lattice. This causes a smoothening of the surface features. A flat Pt(111) surface, devoid of Cr, is regained after prolonged annealing above 770 K. At lower temperatures, metastable Cr−Pt surface alloys are formed. The apparent composition and stability of these surface alloys are dependent upon the amount of Cr deposited initially. Both the Cr adlayer and Pt surface atoms were found to be perturbed at the interface. Experimental and theoretical results indicate that a redistribution of charge between Pt and Cr occurs upon alloy formation with the greatest perturbation experienced by the Pt atoms.

Introduction

An understanding of intermetallic bonding is an important issue for of a wide variety of technological applications. In particular, the study of Pt-containing bimetallic systems is vital in areas related to catalysis and electrochemistry. The hope to design better catalysts and the desire to obtain a predictive understanding of bimetallic bond formation cause an intense research interest in the electronic structure of bimetallic alloys systems.[1] The Pt−Cr system, though interesting from an electrocatalytical viewpoint, has hardly been investigated so far.

We have begun a research program on the growth of ultrathin chromium and chromium oxide films on Pt(111).[2,3] In this paper, we concentrate on one aspect of this study, the thermal stability of ultrathin metallic Cr films on a Pt(111) surface. When ultrathin films are deposited at low temperatures, the growth is often governed by kinetic factors, and metastable phases with unique structural properties may be formed. When the temperature is raised, several phenomena may occur; these include admetal cluster formation or diffusion of the adlayer into the bulk of the substrate which may lead to the formation of surface alloys. These alloys can exhibit chemical and physical properties quite different from those of the supported thin film and bulk systems.

To our knowledge, chromium overlayers on a Pt substrate have not been investigated with surface science techniques previously. The results presented in this paper can be compared with growth of Cr overlayers on other substrates and with other metals on the Pt(111) substrate. There are only a few reports on the thermal properties of ultrathin Cr overlayers on metals. Surface alloying occurs for Cr/Au(001),[4] while Cr overlayers on W(110) and W(100) form three-dimensional clusters with no evidence of alloy formation.[5] Very detailed studies have been undertaken for a wide variety of metal overlayers on Pt.[1] These investigations have been focused on the physical structure[1] and also the electronic structure[6,7] as a function of the adlayer coverage and temperature. The high-temperature behavior of various supported adlayers on Pt has been studied in great detail. Surface alloy formation has been observed for many metal/Pt systems, such as Zn,[6] Cu,[8] Al,[7] Sn,[9] and Co.[10,11] In an accompanying work, we have shown that impinging Cr atoms nucleate at Pt step edges upon initial deposition.[2] Once these sites are saturated, the Cr film grows two-dimensionally across the Pt terraces. For the first two monolayers, the films are found to be pseudomorphic to the Pt(111) substrate. The second layer begins forming before complete wetting by the first layer is observed. Further deposition results in three-dimensional growth and is accompanied by a phase transformation from a strained fcc structure into a bulklike Cr bcc structure. Overall, the growth mode can be described to be that of a modified Stranski−Krastanov type. There was no evidence for alloying or intermixing between Cr and Pt at room temperature. However, since Pt and Cr are completely intermiscible according to their phase diagram,[12] surface alloying or intermixing of the two components is expected at elevated temperatures.

The combination of scanning tunneling microscopy (STM) and low-energy He^+ ion scattering (ISS) gives a very clear picture of the system morphology as the system is annealed. Further information on the change in the geometry of the ultrathin films, upon annealing, and on the electronic modification of the substrate and overlayer is obtained from LEED and XPS measurements, respectively.

With the annealing of Cr ultrathin films on Pt(111), grown at room temperature, we have observed a flattening of the overlayer morphology, a decrease in Cr content at the surface and in the near-surface region, and a significant change in XPS binding energies. These are strong indications for dissolution of Cr into the bulk of the Pt crystal with subsequent alloy formation. These interactions lead to a redistribution of charge between Pt and Cr atoms.

* To whom all correspondence should be addressed. e-mail: mkuhn@mailhost.tcs.tulane.edu.

[⊗] Abstract published in *Advance ACS Abstracts,* May 15, 1997.

S1089-5647(96)02778-2 CCC: $14.00

Experimental Section

The experiments were performed using an ultrahigh-vacuum system, operating at a base pressure of 5×10^{-11} mbar. The system is equipped with capabilities for X-ray photoelectron spectroscopy (XPS), low-energy He^+ ion scattering spectroscopy (LEISS), low-energy electron diffraction (LEED), and scanning tunneling microscopy (STM).

A detailed description of the experimental setup and procedures employed has been given in a previous publication.[2] Therefore, only a brief summary will be given here.

Chromium films were prepared by vapor deposition of Cr from a water-cooled evaporator onto a clean Pt(111) surface at room temperature in ultrahigh vacuum. Sample temperatures were measured using a K-type thermocouple and calibrated to account for a gradient from the sample to the actual point of temperature measurement. During Cr deposition, the base pressure remained below 5×10^{-11} mbar. The growth of the Cr films was monitored by a quartz crystal microbalance. Cr coverages were calibrated using the quartz crystal microbalance and reported with respect to the number of Pt(111) surface atoms (1.51×10^{15} atoms cm^{-2}). One Cr adatom per Pt surface atom corresponds to $\theta_{Cr} = 1$ monolayer (ML). Annealing was performed radiatively via a filament mounted close to the back of the sample plate. Annealing times varied from 5 to 45 min.

Ion scattering spectroscopy and X-ray photoelectron spectroscopy measurements were performed using a cylindrical sector analyzer (CSA) for electron and helium ion detection. For the ISS measurements, 1225 eV incident He^+ ions were scattered through an angle of 137° and collected with a pass energy of 160 eV. The duration of ion exposure on the sample for each spectrum taken was approximately 5 min. XPS measurements were performed at normal electron emission with a pass energy of 20 or 40 eV. Radiation from an unmonochromatized dual-anode (Al and Mg Kα) source with emissions of 1486.6 and 1253.6 eV, respectively, was used. The Pt 4f core levels were also measured at room temperature with a photon energy of 300 eV, using a hemispherical electron analyzer equipped with multichannel detection, at beamline U7A of the National Synchrotron Light Source. The Pt $4f_{7/2}$ and Cr $2p_{3/2}$ core levels were calibrated to known bulk values using the clean Pt(111) sample and a multilayer Cr film on Pt(111). These bulk values are 71.2 and 574.4 eV, respectively.[13]

The LEED measurements were performed at normal electron incidence using retractable rear-view optics. A data acquisition system interfaced with a CCD video camera was employed to acquire the images, thereby allowing for immediate storage and future analysis. Typical beam energies used ranged from 60 to 200 eV.

An in situ sample transfer system allowed for immediate STM characterization of the prepared films. An Omicron UHV STM-1, operated in constant-current mode at room temperature, was used. Chemically etched tungsten tips, with no further treatment except for high voltage−high current pulses during scanning, were employed. Sample bias voltages ranged from −1 to +2 V with tunneling currents of 0.2−3 nA. The *z*-direction was calibrated using the known step height of the Pt(111) surface, namely 2.30 Å.[14]

The ab initio calculations described in the Results section were performed using the HONDO program.[15] Nonempirical effective-core potentials (ECP′S) were used to describe the inner shells of Cr and Pt.[16] The ECP for Pt includes mass−velocity and Darwin relativistic effects.[16] The 4s, 4p, and 3d atomic orbitals of Cr were explicitly treated by a basis set of three s, two p, and five d primitive Gaussian-type orbitals[16] contracted to two s, one p, and two d (3s2p5d/2s1p2d). A basis set obtained through a (3s3p4d/2s1p2d) contraction scheme was used to describe the 6s, 6p, and 5d atomic orbitals of Pt.[6,7] To

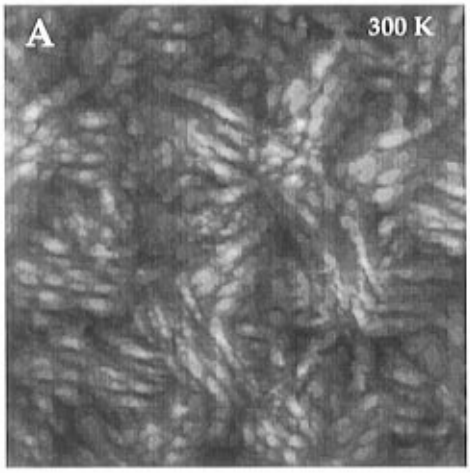

100 nm x 100 nm

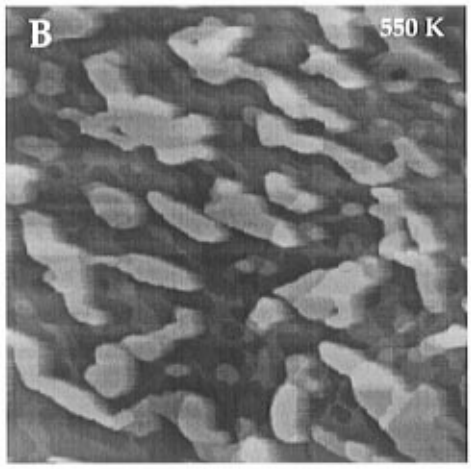

200 nm x 200 nm

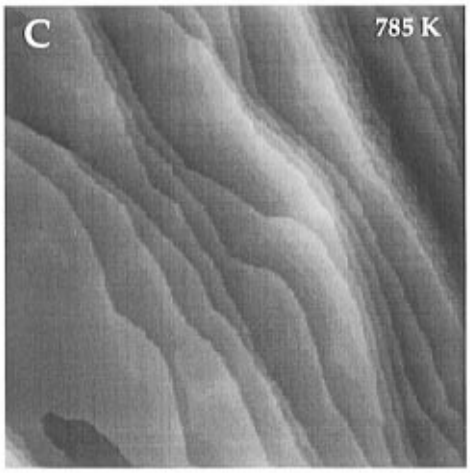

200 nm x 200 nm

Figure 1. Scanning tunneling microscopy (STM) images for a clean Pt(111) surface after the deposition of 5.5 ML of Cr (A). Elongated three-dimensional clusters of Cr are observed with three preferred orientations, 60° to one another. These orientations correspond to the three close-packed directions present on a Pt(111) surface. The Cr step height is 2.1 ± 0.2 Å. A clean Pt(111) surface has a step height of 2.3 ± 0.1 Å (not shown). Parts B and C show STM images of the aforementioned 5.5 ML Cr coverage, which was then successively annealed for ∼45 min to 550 and 785 K, respectively. Comparison of these images reveals a large smoothening of the surface features at 550 K. After annealing to 785 K the surface resembles that of clean Pt(111) (not shown).

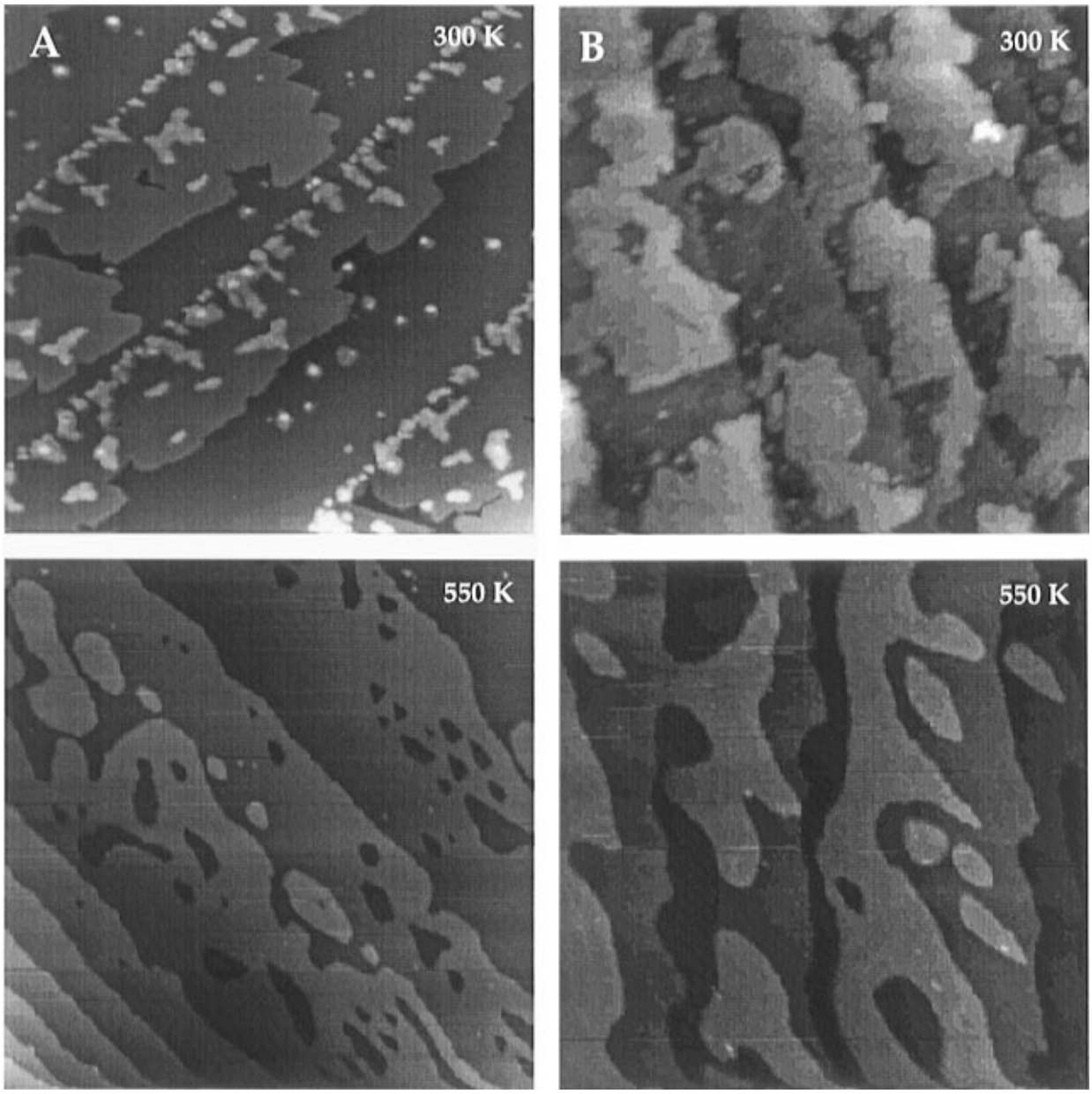

Figure 2. STM images showing the affect of annealing for ~45 min to 550 K on the morphology of two systems: 0.55 ML of Cr (A) and 2.75 ML of Cr (B) on Pt(111). In both cases there is clearly a smoothening of the surface features as a result of the intermixing of the Cr and Pt atoms.

estimate the atomic charges and orbital populations in the bimetallic systems, a Mulliken population analysis was used.[17] Due to the limitations of this type of analysis,[18] the charges must not be interpreted in quantitative terms; therefore, the focus will be on qualitative trends.

Results

STM Results. An STM image of a Pt(111) surface covered with 5.5 ML of Cr at room temperature is shown in Figure 1 along with images of the same coverage annealed to 550 and 785 K. The clean Pt(111) surface exhibits smooth single-stepped terraces ranging in width from less than 100 Å to several hundred angstroms (not shown). In Figure 1A, elongated three-dimensional clusters of Cr, much smaller than the terraces observed for clean Pt(111), are observed. These clusters exhibit average dimensions of 20 Å (width) × 150 Å (length) × 15 Å (height) with the long axis aligned along the close-packed directions of the Pt(111) surface (see LEED results). The average Cr step height was found to be 2.1 ± 0.2 Å.

In Figure 1B,C, STM images of a 5.5 ML Cr/Pt(111) system which has been successively annealed to 550 and 785 K are shown. At 550 K there is an evident reduction in number, and flattening of, the elongated three-dimensional clusters which are present at room temperature. These islands are larger and drop off sharply with straight edges as compared to the more rounded clusters present at room temperature. They are approximately 10 Å high and are the result of the coalescence of the smaller, rougher, three-dimensional islands initially present, a process initiated by the thermally enhanced migration of Cr atoms into the Pt substrate. Figure 1C shows the surface morphology after annealing to 785 K. Flat terraces terminating in single-height atomic steps reappear. The surface is essentially of Pt character since the XPS and ISS results show little Cr remaining in the surface region (see later), and the step height was found to be the same as that of the clean Pt(111) surface.

The morphological changes due to the annealing of 0.55 and 2.75 ML Cr films on Pt(111) to 550 K are shown in Figure 2. The room temperature images show the nucleation of Cr at the Pt step edges at low coverages and the two-dimensional step-flow growth which essentially wets the Pt(111) surface with higher coverages. (See ref 2 for a more detailed description.)

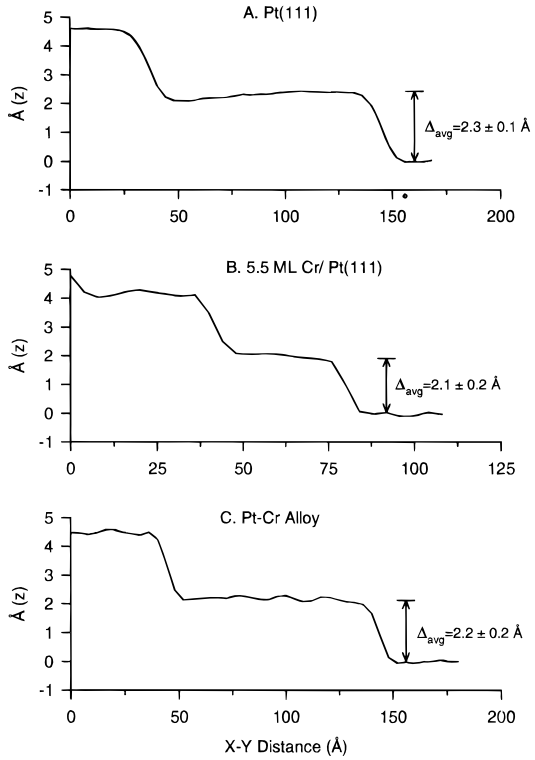

Figure 3. Line profiles taken from STM images shown in Figure 1A (5.5 ML of Cr) and Figure 2 (Pt−Cr surface alloy) and for a clean Pt(111) surface (not shown). The step height values stated are averages taken over various steps in each image with the values normalized to that of the Pt−Pt step height, which was set to 2.3 Å.

After annealing, there is a general smoothening of the surface. The Cr which had nucleated at the Pt step edges has disappeared, presumably migrating into the surface region of the Pt lattice. (See ISS and XPS results later.) In both cases, large two-dimensional islands of a Pt−Cr alloy exist on the surface. The Pt step edges are still evident, although they are not as straight as those exhibited by Cr/Pt(111) systems which have not been annealed. A line profile for an annealed Cr/Pt(111) system is shown in Figure 3. The average step height from a "Pt" region across the alloy was found to be 2.2 ± 0.2 Å, a value between that derived for the Cr−Cr steps and set for the Pt−Pt steps.[14] This value did not vary, within experimental uncertainty, as a function of initial Cr coverage.

ISS and XPS Results. Figure 4 summarizes the ISS results obtained when various coverages of Cr on Pt(111) are annealed in steps from approximately 350 to 900 K. In the left panel the Cr signal was found to decrease for all coverages, upon annealing.[19] A plateau is reached when annealing from 550 to 780 K. With a higher initial Cr coverage, the plateau begins at higher temperatures and Cr concentration. Also, the plateau is more pronounced (flatter) and persists to a higher temperature as the initial coverage is increased. The Cr signal disappears at 800−900 K; the higher the initial Cr coverage, the higher is the temperature at which the Cr signal disappears. The behavior of the Pt signal correlates with these results. The same trends are exhibited with the plateau regions covering the same temperature regime but being less pronounced except at the highest Cr coverage. Two explanations can be invoked to explain the overall decrease (increase) of the Cr (Pt) signals: three-dimensional clustering of Cr exposing the underlying Pt substrate or Cr−Pt alloy formation resulting in the migration of Cr from the surface region into the Pt lattice. The STM results clearly show that clustering is not taking place, and therefore the ISS results can be explained by the migration of the Cr into the Pt lattice. The appearance of the plateau regions indicates the formation of metastable Cr−Pt species whose apparent composition and stability are dependent upon the initial Cr coverage.

Figure 5 shows the ISS results for the high initial coverage of Cr (>10 ML) from Figure 4 along with the corresponding XPS results as a function of annealing temperature. The XPS areas are calculated from the total integrated emissions from the Cr 2p (left) and Pt 4f (right) core levels. Also shown in the right panel of Figure 5 are the Pt $4f_{7/2}$ peak positions. To obtain these values, a simple linear background subtraction was first performed, and then the core levels were iteratively fitted using a Doniach−Sunjic many-body line shape[20] convoluted with a Gaussian function to account for instrumental resolution and phonon broadening. Focusing on the left panel of Figure 5, the Cr ISS and XPS areas correlate closely, with the exception that the plateau region and the initial decrease in the Cr signal are not as pronounced for the Cr XPS results. Both signals disappear after 900 K. Similarly, the Pt XPS signal (bottom panel of Figure 5) also does not exhibit sensitivity to the initial Cr decrease (as exhibited by the ISS results) but does show the plateau region and otherwise correlates well with the Pt ISS signal. The Pt $4f_{7/2}$ peak position, for this coverage, shifts continuously toward higher binding energy as the temperature is increased until ∼850 K, at which point there is a dramatic decrease, and by 950 K a bulk Pt binding energy position is reached.[21] This decrease in binding energy corresponds with the large increase in the Pt ISS and XPS signal areas. Two points to be noted are (1) Pt experiences a small positive binding energy shift upon initial Cr deposition and (2) there is no evidence of a plateau region in the plot of binding energy shift versus annealing temperature. For these high coverages, the Cr 2p core levels did not exhibit significant shifts upon annealing.

The Cr $2p_{3/2}$ and Pt $4f_{7/2}$ core level positions as a function of temperature for two different initial Cr coverages are given in the top of Table 1. Small binding energy shifts are evident in both core levels upon annealing, especially for the Pt site. Also, there is a coverage-dependent shift in both the Cr and Pt core levels. Of particular interest is the disappearance of the Cr signal after a 2.75 ML Cr film has been annealed to 785 K. Also, the Cr emission has been greatly attenuated after annealing a 5.5 ML Cr film to the same temperature. Because of the larger sampling depth by XPS versus ISS, this indicates that, upon annealing, the Cr migrates into the Pt substrate leading to the formation of Cr−Pt alloys. In the bottom of Table 1, high-resolution synchrotron-based photoemission results are shown for the Pt $4f_{7/2}$ core level for a low and high coverage of Cr at room temperature. Again, these results indicate a small shift in the Pt core levels upon the deposition of Cr.

LEED Results. The LEED results for the annealing of a multilayer Cr coverage (>5 ML) are summarized in Figure 6. At room temperature the Cr exhibits a complex pattern. This pattern is the result of the Cr multilayer adopting an bulklike bcc(110) structure but oriented with six domains due to the influence of the Pt substrate.[2] As the temperature is increased, the satellite spots gradually disappear, and only a hexagonal (1 × 1) pattern remains at 780 K. There is evidence of a faint (2 × 2) pattern at these high temperatures, presumably due to a small amount of oxygen contamination which results in the formation of the thermally more stable Cr_3O_4 species.[3] Using the previous ISS and XPS results, it can be concluded that the primary spots at elevated temperatures are those due to a Pt-(111) surface devoid of the presence of Cr.

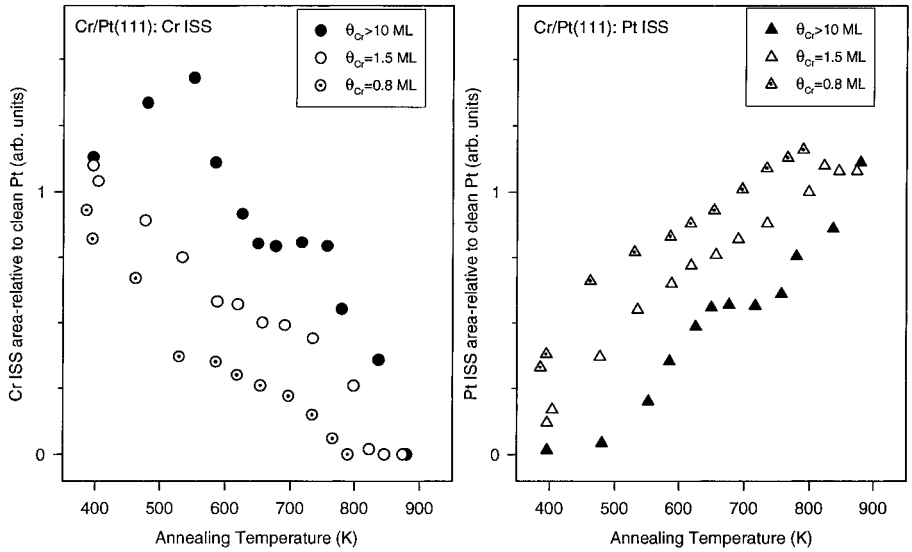

Figure 4. Ion scattering spectroscopy (ISS) results for various coverages of Cr on Pt(111) as a function of annealing temperature (annealing time was ~5 min per data point). The areas of both the Cr (left) and Pt (right) ISS peaks are measured relative to the ISS peak area of a clean Pt(111) surface. Note the presence of plateau regions for all of the coverages in both the Cr and Pt ISS signals.

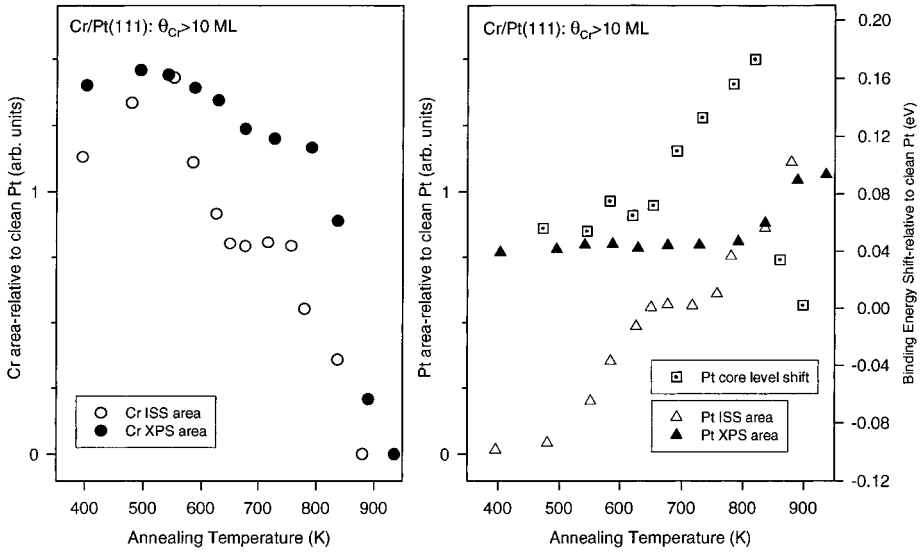

Figure 5. Comparison of the ISS and X-ray photoelectron spectroscopy (XPS) results for a multilayer Cr coverage on Pt(111) as a function of annealing temperature (annealing time was ~5 min per data point). The Cr results (left) and Pt results (right) clearly show a strong correlation of the ISS and XPS areas. In the case of Cr the area of the Cr 2p core levels were measured while for Pt the area of the Pt $4f_{7/2}$ core level was employed. Also included in is the Pt $4f_{7/2}$ core level shift as measured with respect to the clean Pt(111) surface (right). There is an initial shift toward higher binding energy with a collapse to the bulk Pt value after 800 K is reached. This corresponds to the disappearance of both the XPS and ISS Cr signal (left of figure).

Electronic Interactions in Cr/Pt(111) Surfaces. Figure 7 shows the clusters used to study the bonding interactions between Cr and Pt. Previous studies indicate that metal clusters of this size can provide a very good qualitative picture of the interactions that occur in bimetallic systems, with results that agree with those seen in band-structure calculations for bulk alloys and metal−metal interfaces.[1,22−25] Here, a Cr/Pt_9 cluster models the adsorption of Cr on a hollow site of Pt(111) (cluster I). The Pt−Pt distances were set equal to those observed in the bulk metal.[26] The Cr−Pt separation was optimized at the ab initio SCF (self-consistent field) level, obtaining a value of 2.61 Å for the ground state of the cluster. To model the interactions in Cr−Pt alloys, a Cr_4Pt_4 cluster was used (cluster II). For this system, the ab initio SCF calculations showed Pt−Cr optimal distances of 2.58 Å in the ground state. This value is close to that found for the Cr/Pt_9 cluster and somewhat shorter than the corresponding sum of the metallic radii (2.67 Å[26]).

Table 2 lists calculated charges and orbital populations for the Cr/Pt_9 and Cr_4Pt_4 clusters. For comparison, the corresponding values for homonuclear Cr_8, Pt_9, and Pt_8 clusters are also shown. In the bimetallic system there is a small net charge transfer (~0.1*e*) from Cr to Pt. Among the metals, Pt has the largest electron affinity.[27] When a Cr−Pt bond is formed, both metal centers lose some type of charge. The Pt atoms in the Cr/Pt_9 and Cr_4Pt_4 clusters show a substantial reduction in the electron population of the 5d orbitals and an increase in the population of the (6s,6p) orbitals. This type of behavior is consistent with the results of previous theoretical and experimental studies,[28−31] which show that Pt can act as a 5d-electron donor and a (6s,6p)-electron acceptor when forming compounds. The change in the relative populations of the Pt(5d,6s,6p) orbitals is equivalent to a d → s,p rehybridization. This rehybrization shifts d electrons from around the Pt centers into regions around the bimetallic bonds.

TABLE 1: XPS Results for Two Cr Coverages, 2.75 and 5.5 ML, as a Function of Annealing Temperature (Top) and Synchrotron Photoemission Results for Various Coverages at Room Temperature (Bottom)

Photon Energy: 1486.6 or 1253.6 eV

θ_{Cr}	temp (K)	Pt $4f_{7/2}$ (±0.1 eV)	Cr $2p_{3/2}$ (±0.2 eV)
2.75	300	71.25 (2.10)[a]	574.10 (2.60)
	620	71.45 (2.05)	574.15 (2.70)
	785	71.20 (2.05)	
5.5	300	71.25 (2.05)	574.40 (2.30)[b]
	620	71.40 (2.00)	574.25 (2.70)
	785	71.25 (2.10)	574.40 (3.30)

Photon Energy: 300 eV

θ_{Cr}	temp (K)	Pt $4f_{7/2}$ (±0.05 eV)
0	300	71.20 (1.1)
<1	300	71.25−71.30 (0.95)
∼5	300	71.28 (1.2)

[a] Values in parentheses are the fwhm of the fitted peaks. [b] The relative areas of the Cr $2p_{3/2}$ peaks are 6:4:1 at 300, 620, and 785 K, respectively.

In summary, these results indicate that Cr films supported on Pt(111) gradually intermix with the Pt surface and continue migrating into the bulk at elevated temperatures. They form metastable phases, the apparent composition of which are dependent upon the initial concentration of Cr. Neither LEED nor STM is able to reveal any structural information on these metastable phases. Experimental and theoretical results show that both the Pt and Cr sites are electronically perturbed upon contact and alloy formation with the greatest perturbation experienced by the Pt atoms.

Discussion

Chromium adopts a bcc structure in the bulk while Pt adopts an fcc structure. Both elements are miscible in the bulk with the phase diagram exhibiting a large solid solution region.[12] The existence of three superlattice structures, Cr_3Pt, CrPt, and $CrPt_3$, has also been postulated.[12] The surface free energy of Cr is less than that of Pt, leading one to expect that Cr will wet the Pt substrate, at least in the first monolayer.[32] However, theoretical estimates based on Miedema's model have shown that there is a large negative heat of solution for Cr dissolved in Pt and Pt dissolved in Cr.[32] This suggests that there is a large driving force for alloy formation between these two elements. These results confirm this expectation and show that alloying occurs in the Cr/Pt(111) system at temperatures as low as 400−500 K.

Thermal Stability: Morphological and Compositional Aspects. Recent results have shown that the first two layers of Cr grow two-dimensionally and pseudomorphic to the Pt(111) surface at room temperature.[2] Further deposition of Cr results in the appearance of a bulklike bcc(110) structure, indicating that Cr adopts the stable surface-terminated bulk bcc structure. There was little evidence for alloying at room temperature.

Upon annealing, the Cr atoms gradually diffuse into the Pt lattice. This thermally enhanced diffusion leads to the formation of smooth two-dimensional features regardless of the initial Cr coverage. At low coverages, Cr clusters that have nucleated at the Pt step edges at room temperature spread across the Pt terrace as intermixing occurs. These alloys appear homogeneous. At larger coverages, annealing the Cr overlayers also leads to smoothening of the surface features and formation of a homogeneous alloy. The three-dimensional Cr clusters break down with the Cr located at the interface with the Pt(111) surface forming a Cr−Pt alloy and the remaining unreacted Cr sitting on top of this alloy. Close examination of Figure 1A reveals the smooth appearance of the surface between the clusters. These features resemble that seen for lower coverages of Cr annealed to 550 K (Figure 2). The exposure of the surface (interface) and the unchanged height (perhaps even a small decrease) of the remaining Cr clusters clearly indicates the loss of Cr from the surface. The clusters themselves appear very flat with sharp, straight edges. This boxlike shape is due to the thermally enhanced mobility of the supported Cr atoms which allows for the formation of the lowest energy crystal faces (110) of a bcc lattice. These faces are at 90° to one another. Only after annealing to higher temperatures does one react the remaining Cr and regain an overall morphology typical of that of the annealed low coverages of Cr. In all cases, prolonged annealing to greater than 785 K results in the reappearance of a clean Pt(111) surface. This behavior for Cr on Pt(111) is contrary to that found for Cr on W(110) and W(100) where the Cr adatoms formed three-dimensional clusters on these surfaces and eventually desorbed at temperatures above 1200 K.[5] Calculations have shown that Cr dissolved in W and W dissolved in Cr display positive heats of solution (i.e., nonfavorable for alloying) consistent with the previously reported experimental results.[32]

Both ISS and XPS results reveal the presence of metastable Cr−Pt alloys from ∼550 to 780 K. The presence of these alloys is more apparent from ISS measurements. The sampling depth for ISS is restricted to the surface layer while XPS probes further into the bulk. Therefore, the XPS signal is strongly convoluted with bulk emissions, especially with those from unreacted Pt. Combining these observations with the fact that the Pt $4f_{7/2}$ core level shift does not exhibit a plateau, it can be concluded that the metastable alloy is localized in the surface region. These alloys also exhibit a flatter plateau and greater thermal stability as the initial amount of Cr deposited is increased. Also, as the initial Cr coverage is increased, the Cr concentration in the metastable alloy increases. At the highest Cr coverage examined here, the resultant metastable phase has a 1:1 Cr−Pt composition. Those alloys formed with a lower initial Cr deposition are not as stable and exhibit an overall composition ranging from 20 to 30% Cr in the surface layer. However, one cannot dismiss the possibility that these surface alloys also have a 1:1 composition and that the lower apparent Cr concentration, relative to Pt, is due to the exposure of a higher amount of unreacted Pt surface atoms (i.e., islands of a 1:1 Pt−Cr alloy distributed on the clean Pt(111) surface). This assumption implies that a certain subsurface Cr concentration must be reached in order to stabilize the surface alloy. Evidence for this comes from noting that even the lowest coverage of Cr studied here (0.8 ML) does not immediately form a complete 1:1 surface alloy even though there are enough Cr atoms present. LEED results do not indicate the formation of a superlattice structure with any long-range order. The persistence and invariance in position of the Pt hexagonal 1×1 pattern indicates that the *interdiffusing* Cr atoms do not induce a phase transformation to a bcc structure in the near surface region nor adopt such a structure at any Cr concentration. This may imply that the Pt−Cr species never form alloys with higher than a 50% Cr concentration. The STM results do not reveal any specific morphology associated with the presence of these metastable surface alloys.[33]

Electronic Interactions between Cr and Pt. The electronic interactions of various metals with Pt has been examined in detail both experimentally[1] and through theoretical calculations.[6,7] Typically, Pt experiences a redistribution of charge which leads to an overall depletion of d character with a

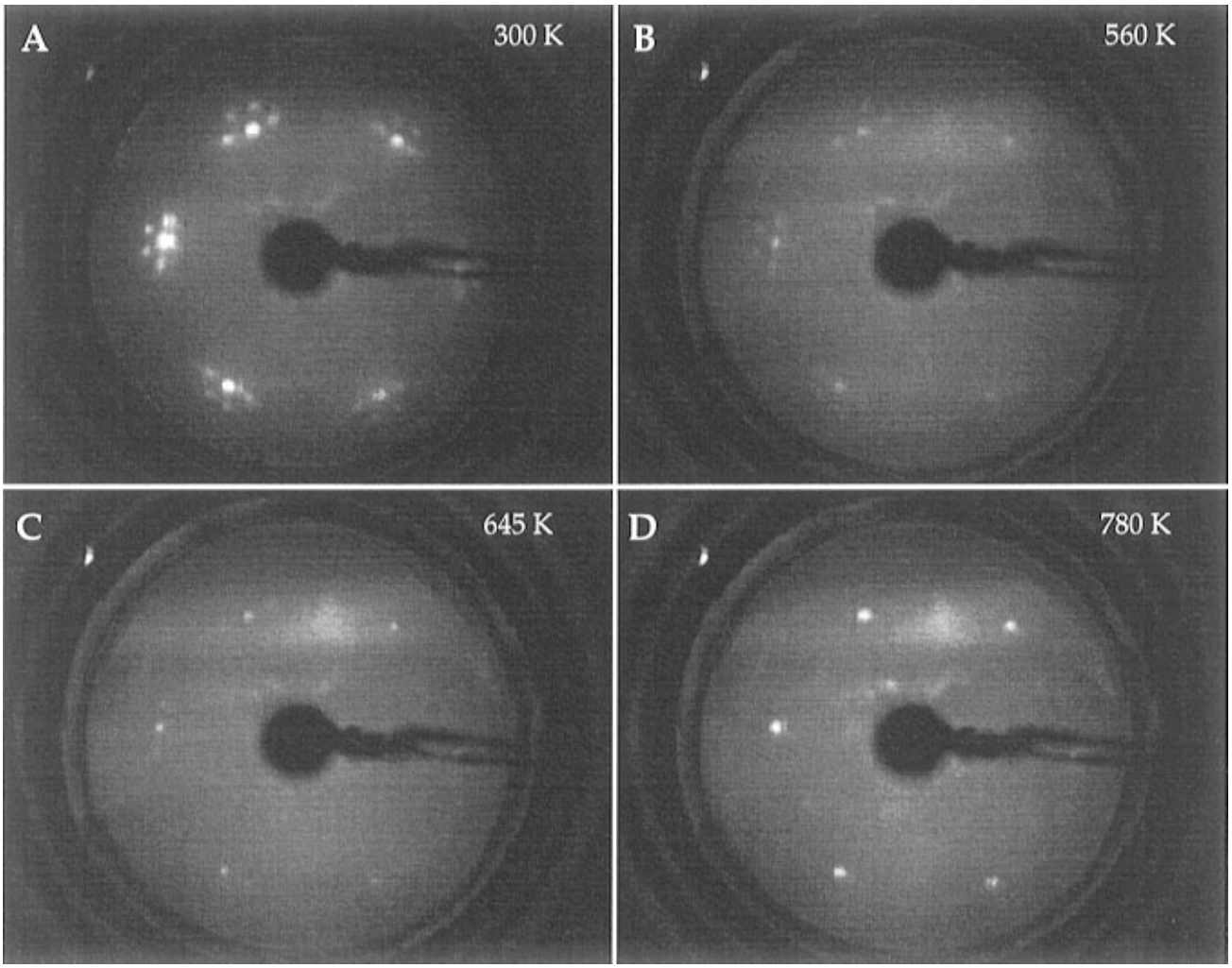

Figure 6. Low-energy electron diffraction (LEED) results for 5.5 ML coverage of Cr on Pt(111) as a function of annealing temperature. The room temperature results (A) reveal the presence of an unrelaxed Cr bcc(110) surface, the satellite spots being produced by alignment of the noncommensurate bcc(110) unit cell with the underlying Pt(111) surface. As the temperature is increased, the satellite spots begin to disappear, and by 780 K only a hexagonal 1 × 1 structure is observed. This reflects the presence of a Pt(111) surface devoid of Cr.

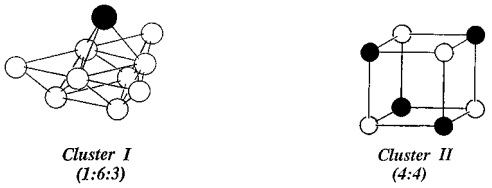

Figure 7. Clusters employed to study the interaction between Cr atoms (closed circles) and Pt atoms (open circles). Cluster I represents the adsorption of Cr on the center of a fcc hollow site of Pt(111). Cluster II has a cubic configuration and was used to model metal−metal bonding in 1:1 Cr−Pt alloys.

corresponding increase in s−p character.[6,7] This redistribution of charge is largest when the other metal has a valence band that is less than half full.[6,7] The electronic interactions of Cr with other metals has not been extensively studied with the exception of the systems Cr/Cu(100) and Cr/Ag(100).[34] In both cases the Cr core levels were at lower binding energy as compared to bulk Cr with the Cr/Ag(100) system exhibiting the larger negative binding energy shift.[34]

The XPS and synchrotron-based photoemission results (Figure 6 and Table 1) show that upon deposition of Cr on Pt(111) there is a small initial shift (∼0.05−0.10 eV) toward *higher binding* energy for the Pt $4f_{7/2}$ peak. As the system is annealed, the peak position remains constant until a temperature of ∼650 K is reached, at which point a further shift toward higher binding energy is observed. A maximum shift of ∼0.2 eV is found at 800 K, at which point the peak position is sharply reduced and a bulk Pt peak position is observed at 900 K. This behavior correlates with the rapid dissolution of Cr into the bulk of Pt at elevated temperatures as observed by XPS and ISS intensities and STM measurements.

Surface atoms on Pt(111) display a binding energy value ∼0.3 eV smaller than that of the bulk.[28] Using this result and the

TABLE 2: Results of Molecular-Orbital Calculations for a Series of Cr−Pt Heteronuclear and Cr and Pt Homonuclear Clusters as Shown in Figure 7

Chromium Orbital Populations (Electrons)				
cluster	3d	4s	4p	charge
Cr/Pt_9	5.18	0.66	0.04	0.12
Cr_4Pt_4[a]	5.24	0.60	0.07	0.09
Cr_8[a]	5.21	0.75	0.04	0.00
Platinum Orbital Populations (Electrons)				
Pt_9[b]	9.31	0.68	0.07	−0.06
Cr/Pt_9[b]	9.13	0.92	0.06	−0.11
Cr_4Pt_4[c]	9.16	0.75	0.18	−0.09
Pt_8[c]	9.37	0.51	0.12	0.00

[a] The values reported are for one of the Cr atoms, which are all equivalent in these clusters. [b] The values listed are for one of the Pt atoms that form the adsorption site. [c] The values reported are for one of the Pt atoms, which are all equivalent in these clusters.

fact that in this system a small overall positive core level shift is experienced, even though emissions are dominated by bulk contributions, leads to the conclusion that the surface Pt atoms are highly perturbed by the Cr overlayer. After annealing, with Cr diffusing into the Pt lattice, a shift to higher binding energy is observed. This is due to the formation of a Cr−Pt alloy and also due to the fact that the emissions are increasingly dominated by the formation of thicker and thicker Cr−Pt alloys. The behavior of the Pt atoms in this system is typical of that observed for a number of Pt bimetallics.[6,7] Pt has a much higher electronegativity (and electron affinity) than does Cr. One would then expect a gain of charge and hence an increase in the electron−electron repulsion at the Pt site. This is corroborated by the results of the ab initio SCF calculations for Cr/Pt_9 and Pt_4Cr_4 clusters (see Table 2; total charge for Cr and Pt). This should lead to a reduced Coulombic interaction with the nucleus and a shift of the electronic levels toward *lower binding* energy. However, it has been demonstrated that one must take into account not only the net charge transfer but also the nature of that charge.[6,7] Pt has been shown to lose d electrons but experience a net gain of charge by an overcompensation of s−p charge in bimetallic systems. This gain of s−p charge can be rationalized through a mechanism of charge transfer from the other metal or bonding-induced rehybridization of the Pt valence levels (5d → 6s−p). Because of the larger screening ability of d electrons (as compared to s−p electrons), an equivalent loss of d and gain of s−p charge at the Pt site would result in a net higher Coulombic interaction with the nucleus and a shift of the electronic levels toward higher binding energy. This is the phenomenon experienced by the Cr−Pt system as shown by the experimental positive core level shifts at the Pt site. Similarly, the theoretical cluster calculations indicate the loss of d charge with an overcompensation of s,p charge in agreement with these arguments (see Table 2; Pt 5d, 6s, and 6p orbital populations).

The electronic interactions at the Cr site in these alloys are not as straightforward to deduce. The Cr core levels are inherently broad and nonsymmetrical, not allowing for an easy determination of binding energy shifts. In Table 1 the XPS results are shown for two coverages of Cr on Pt(111) annealed to 620 and 785 K. A 2.75 ML coverage of Cr shows a binding energy value for the Cr $2p_{3/2}$ core level which is ∼0.3 eV below that of bulk Cr. The core level shift of the thin, pseudomorphic layer in contact with the Pt substrate should be referenced to the value for Cr surface atoms on a Cr crystal, but this value is not known. However, the direction for the coverage-dependent shift is the same as that seen for Cr on Cu(100) and Ag(100) where the values were reported as −0.3 and −1.0 eV, respectively, upon initial deposition.[34] The differences were attributed solely to the fact that there is a three-dimensional growth mechanism on Cu(100) versus a two-dimensional mechanism on Ag(100).[34] Since Cr on Pt(111) also grows two-dimensionally, the dissimilarity with the Cr/Ag(100) system must be due to the significant influence of the Pt substrate as compared to a relatively noninteracting Ag substrate. Therefore, one can conclude that the Cr electronic levels also experience a positive core level shift when in contact with Pt. After annealing, there is a further shift toward higher binding energy for the core levels of a 2.75 ML Cr coverage. For multilayer coverages, the effect of annealing on the Cr electronic levels is harder to see. For example, in Table 1 a 5.5 ML Cr coverage displays a bulk Cr value at 300 K which shifts slightly lower after annealing to 620 K. The STM results show that the three-dimensional Cr islands had coalesced into two-dimensional structures with a significant amount of Cr still not alloyed with Pt. This convolutes the Cr signal with contributions from Cr alloyed to Pt and Cr surface atoms supported on this alloy making an exact peak assignment difficult. After annealing this multilayer coverage to 785 K, a small broad Cr signal remains, displaying a binding energy value close to that of bulk Cr. This behavior for the multilayer Cr coverages may account for the reason that no significant Cr shifts were seen for the multilayer system of Figure 6 as a function of anneal temperature. It is also worthy to note that the theoretical cluster calculations do not show significant charge redistribution in the Cr orbitals especially for the 3d levels. However, the calculations do show a small net loss of charge at the Cr site in line with simple electronegativity arguments.

In summary, both the Pt and Cr electronic levels experience perturbations upon contact and alloying. These electronic interactions are complex. The Pt atoms experience a loss of d charge and an overcompensation of s−p charge through a charge transfer and/or a charge rehybridization mechanism. The electronic interactions at the Cr site are difficult to interpret within experimental uncertainties, and they may also be inherently insignificant.

Conclusions

1. Ultrathin Cr films supported on Pt(111) decompose upon annealing with the Cr atoms diffusing into the Pt lattice. During this process metastable surface alloys are formed. The apparent composition and thermal stabilities exhibited by these metastable phases depends on the initial Cr coverage.

2. Both the Cr and Pt sites were found to be electronically perturbed upon initial Cr deposition and subsequent alloy formation. The largest perturbation was experienced by the Pt site. There is a complex charge redistribution leading to a net rehybridization of the Pt valence levels (5d → 6s−p).

Acknowledgment. The work performed at Tulane University was supported by LEQSF(1994-97)-RD-A-26, the Petroleum Research Fund, the Center for Photoinduced Processes (NSF-EPSCoR), and DOE-EPSCoR. The work performed at Brookhaven National Laboratory was supported under Contract DE-ACo2-76CH00016 with the U.S. Department of Energy, Office of Basic Energy Sciences, Chemical Science Division.

References and Notes

(1) Rodriguez, J. A. *Surf. Sci. Rep.* **1996**, *24*, 223.
(2) Zhang, L. P.; Kuhn, M.; Diebold, U. *Surf. Sci.* **1997**, *371*, 223.
(3) Zhang, L. P.; Kuhn, M.; Diebold, U. *Surf. Sci.*, in press.
(4) Hanf, M. C.; Pirri, C.; Peruchetti, J. C.; Bolmont, D.; Gewinner, G. *Phys. Rev. B* **1989**, *39*, 3021.
(5) Berlowitz, P. J.; Shinn, N. D. *Surf. Sci.* **1989**, *209*, 345.
(6) Rodriguez, J. A.; Kuhn, M. *J. Chem. Phys.* **1995**, *102*, 4279.
(7) Rodriguez, J. A.; Kuhn, M. *Chem. Phys. Lett.* **1995**, *240*, 435.
(8) Belkhou, R.; Barrett, N. T.; Guillot, C.; Fang, M.; Barbier, A.; Eugène, J.; Carrière, B.; Naumovic, D.; Osterwalder, J. *Surf. Sci.* **1993**, *297*, 40.
(9) Overbury, S. H.; Ku, Y.-S. *Phys. Rev. B* **1992**, *46*, 7868.
(10) Atrei, A.; Bardi, U.; Galeotti, M.; Rovida, G.; Torrini, M.; Zanazzi, E. *Surf. Sci.* **1995**, *339*, 323.
(11) Thiele, J.; Barrett, N. T.; Belkhou, R.; Guillot, C.; Koundi, H. *J. Phys.: Condens. Matter* **1994**, *6*, 5025.
(12) Hansen, M. Constitution of Binary Alloys. In *Constitution of Binary Alloys*, 2nd ed.; McGraw-Hill: New York, 1958; p 553.
(13) Moulder, J. F.; Stickle, W. F.; Sobol, P. E.; Bomben, K. D. Handbook of X-ray Photoelectron Spectroscopy. In *Handbook of X-ray Photoelectron Spectroscopy*; Chastain, J., Ed.; Perkin-Elmer: Eden Prairie, MN, 1992.
(14) MacLaren, J. M.; Pendry, J. B.; Rous, P. J.; Saldin, D. K.; Somorjai, G. A.; Hove, M. A. V.; Vvedensky, D. D. *Surface Crystallographic Information Service: A Handbook of Surface Structures*; D. Reidel: Dordrecht, Holland, 1987.

(15) Dupuis, M.; Chin, S.; Marquez, A. Relativistic and Electron Correlation Effects in Molecules and Clusters. In *NATO ASI Series*; Malli, G. L., Ed.; Plenum: New York, 1992.

(16) Hay, P. J.; Wadt, W. R. *J. Chem. Phys.* **1985**, *82*, 270.

(17) Mulliken, R. S. *J. Chem. Phys.* **1955**, *23*, 1841.

(18) Szabo, A.; Ostlund, N. S. Modern Quantum Chemistry. In *Modern Quantum Chemistry*; McGraw-Hill: New York, 1989.

(19) The intensity of ISS is very sensitive to small amounts of impurities adsorbed on surfaces, especially hydrogen. Desorption of such impurities may account for the fact that the Pt signals in Figure 4 are higher after annealing than before the Cr deposition. This may also cause the initial increase observed for the Cr signal from a Cr multilayer in the left panel of Figure 4, although a smoothening of the surface morphology may also play a role.

(20) Doniach, S.; Sunjic, M. *J. Phys. C* **1970**, *3*, 285.

(21) If one compares the results shown in Table 1 with that of Figure 5, it is found that the onset for the Pt core level shift is at lower temperature (i.e., a 0.2 eV is found at 620 K, while in Figure 5 a similar shift is not seen until ∼800 K) for the coverages listed in Table 1. The early onset of the Pt core level shift is due to the fact that the coverages listed in Table 1 had been annealed for ∼45 min versus the multilayer in Figure 5 in which the annealing times between data points was only 5 min. Enhanced diffusion and intermixing have occurred for the coverages listed in Table 1 and, hence, resulted in increased alloy formation and larger Pt core level shift for the same temperature.

(22) Rochefort, A.; Fournier, R. *J. Phys. Chem.* **1996**, *100*, 13506.

(23) Rodriguez, J. A. *Surf. Sci.* **1996**, *345*, 347.

(24) Castellani, N. J.; Legare, P. *J. Phys. Chem.* **1994**, *98*, 9606.

(25) Ferullo, R. M.; Castellani, N. J. *Langmuir* **1996**, *12*, 70.

(26) Kittel, C. Introduction to Solid State Physics. In *Introduction to Solid State Physics*; Wiley: New York, 1986; pp 24, 76.

(27) Emsley, J. The Elements. In *The Elements*; Clarendon Press: Oxford, 1990; p 231.

(28) Apai, G.; Baetzold, R. C.; Jupiter, P. J.; Viescas, A. J.; Lindau, I. *Surf. Sci.* **1983**, *134*, 122.

(29) Jeon, Y.; Chen, J.; Croft, M. *Phys. Rev. B* **1994**, *50*, 6555.

(30) Horsley, J. A. *J. Chem. Phys.* **1982**, *76*, 1451.

(31) Hay, P. J. *J. Am. Chem. Soc.* **1981**, *103*, 1390.

(32) Miedema, A. R. *Z. Metallk.* **1978**, *69*, 455.

(33) In certain cases, under very specific conditions (Cr concentration and annealing time and temperature) atomic-scale images of a two-dimensional Cr−Pt surface alloy were obtained. The structure is quite complicated and unique however, and a solid interpretation is being worked on at the moment. A discussion of this observation would go beyond the scope of the current paper.

(34) Rouyer, D.; Krembel, C.; Hanf, M. C.; Bolmont, D.; Gewinner, G. *Surf. Sci.* **1995**, *331*−*333*, 957.